Computers & Geosciences 103 (2017) 204–214

Contents lists available at ScienceDirect

Computers & Geosciences

journal homepage: www.elsevier.com/locate/cageo

Research paper

A 3-D wellbore simulator (WELLTHER-SIM) to determine the thermal diffusivity of rock-formations

J.A. Wong-Loya[a,b], E. Santoyo[a,c,*], J. Andaverde[d]

[a] Instituto de Energías Renovables, Universidad Nacional Autónoma de México, Priv. Xochicalco s/n, Col. Centro, Temixco, Morelos 62580, Mexico
[b] Colegio de Ciencias y Humanidades, Plantel Vallejo, Universidad Nacional Autónoma de México, Av. Cien Metros s/n, Col. Magdalena de las Salinas, Distrito Federal 07760, Mexico
[c] Centro de Investigación en Ingeniería y Ciencias Aplicadas, Universidad Autónoma del Estado de Morelos, Av. Universidad 1001, Chamilpa, Cuernavaca 62100, Morelos, Mexico
[d] Centro de Investigación en Recursos Energéticos y Sustentables, Universidad Veracruzana, Av. Universidad Veracruzana Km. 7.5, Coatzacoalcos, Veracruz 96538, Mexico

ARTICLE INFO

Keywords:
Geothermal energy
Thermophysical properties
Heat transfer
Drilling and completion
Statistics
Petroleum

ABSTRACT

Acquiring thermophysical properties of rock-formations in geothermal systems is an essential task required for the well drilling and completion. Wellbore thermal simulators require such properties for predicting the thermal behavior of a wellbore and the formation under drilling and shut-in conditions. The estimation of static formation temperatures also needs the use of these properties for the wellbore and formation materials (drilling fluids and pipes, cements, casings, and rocks).

A numerical simulator (WELLTHER-SIM) has been developed for modeling the drilling fluid circulation and shut-in processes of geothermal wellbores, and for the *in-situ* determination of thermal diffusivities of rocks. Bottomhole temperatures logged under shut-in conditions (BHT_m), and thermophysical and transport properties of drilling fluids were used as main input data. To model the thermal disturbance and recovery processes in the wellbore and rock-formation, initial drilling fluid and static formation temperatures were used as initial and boundary conditions. WELLTHER-SIM uses these temperatures together with an initial thermal diffusivity for the rock-formation to solve the governing equations of the heat transfer model. WELLTHER-SIM was programmed using the finite volume technique to solve the heat conduction equations under *3-D* and transient conditions. Thermal diffusivities of rock-formations were inversely computed by using an iterative and efficient numerical simulation, where simulated thermal recovery data sets (BHT_s) were statistically compared with those temperature measurements (BHT_m) logged in some geothermal wellbores.

The simulator was validated using a well-documented case reported in the literature, where the thermophysical properties of the rock-formation are known with accuracy. The new numerical simulator has been successfully applied to two wellbores drilled in geothermal fields of Japan and Mexico. Details of the physical conceptual model, the numerical algorithm, and the validation and application results are outlined in this work.

1. Introduction

Thermophysical properties of rocks are crucial to study the thermal evolution of crust and lithosphere, magma chambers, upper-mantle rocks, geothermal and petroleum systems (Wohletz et al., 1999; Whittington et al., 2009; Cloetingh et al., 2010). Heat transfer and the anisotropy of thermal diffusivities in the upper mantle control the Earth´s dynamics, whereas the thermal conductivity of rocks is vital to estimate terrestrial heat flows (Tommasi et al., 2001; Gibert, 2003; Bording et al., 2016). The study of heat transfer in the drilling of geothermal wells is needed for the evaluation of heat reserves. The analysis of temperature logs is useful for the location of permeable zones in the wellbore where fluids and/or heat may be lost or gained from the formation. The estimation of static formation temperatures (SFT) also requires the use of thermophysical properties for the wellbore and rock materials (Zhou et al., 2015). Temperature distribution of heat conduction processes, which also depends on thermophysical properties, is a key parameter to predict the thermal evolution of the wellbore and rock-formation.

Wellbore simulators are still developed for the prediction of thermal processes under drilling and shut-in conditions (e.g., Espinosa-Paredes et al., 2001; Yang et al., 2013; Wu et al., 2014; Li

* Corresponding author at: Instituto de Energías Renovables, Universidad Nacional Autónoma de México, Priv. Xochicalco s/n, Col. Centro, Temixco, Morelos 62580, Mexico.
E-mail address: esg@ier.unam.mx (E. Santoyo).

http://dx.doi.org/10.1016/j.cageo.2017.03.016
Received 4 July 2016; Received in revised form 16 March 2017; Accepted 21 March 2017
Available online 27 March 2017
0098-3004/

et al., 2015; Liu et al., 2016). Some simulators use heat conduction and convection models together with bottomhole temperatures (BHT_m) and thermophysical properties of solid and fluid materials. BHT_m measurements are easily acquired from well logging (under shut-in); whereas thermophysical properties are more difficult to get owing to the lack of cores or representative rock samples from outcrops.

Transport and thermophysical properties of drilling fluids are needed to study heat convection processes, especially when lost circulation occurs during the wellbore drilling (García et al., 1998). Experimental methodologies have been reported for the measurement of these properties (e.g., Kiyohashi et al., 1996; Santoyo et al., 2001; Weirich et al., 2001). Fluid viscosity is one of the most important properties affecting heat convection, whereas density and heat capacity have less importance (Santoyo et al., 2003). Thermal conductivity of drilling fluids depends on temperature, although some works report that this dependence may be weak under drilling (Hoang, 1980). Thermal conductivity and diffusivity of rocks are also required for studying the thermal evolution of a wellbore before and after the thermal disturbance caused by the fluid circulation.

Thermophysical properties of rocks can be measured either at the lab or under *in-situ* conditions. The experimental measurement is a complex task due to the sample anisotropy properties (porosity, permeability, microstructures, deformation, stratification, and geometry) and the heterogeneous composition (Fuchs et al., 2015). *In-situ* determinations are more difficult, costly and less accurate than those methods carried out at the lab under controlled conditions (Bording et al., 2016). Ricard et al. (2011) pointed out that the inherent complexity of rocks causes a difficulty to the interpretation of data logged from direct measurements. To overcome these issues, the installation of tools in wells and lab experiments to limit the variability of rocks' thermal properties is suggested. Although, it is also known that some experimental difficulties to measure *in-situ* thermal conductivity and diffusivity still exist due to the lack of downhole temperature probing, and the scarce of wellbore drilling information. Techniques based on steady-state and transient divided bar, hot-wire, and line-source methods are available for the measurement of thermophysical properties of rocks (e.g., Sass et al., 1984; Vosteen and Schellschmidt, 2003). Numerous techniques exist for the measurement of thermal conductivity of rocks whereas for thermal diffusivity are scarce (Beck, 1988; Ricard et al., 2011). Some unsatisfactory results of thermal diffusivity measurements in rocks are reported due to the sample heterogeneities (Arias-Penas et al., 2015). Experimental errors up to 6% have been reported for upper mantle rocks, and mostly attributed to contact probe instruments (Bording et al., 2016). Although these errors are acceptable, differences up to 30% are found when these measurements are compared with theoretical models and inverse methods (Gibert, 2003). These differences are attributed to microfractures and lattice imperfections of the samples. Temperature and pressure changes are also factors that may affect the measurement of these properties due to the variation of porosity, permeability and saturation (Krishnaiah et al., 2004). As variability, a factor up to three times is reported even for the same rock type (Sundberg et al., 2009). In response to these sources of variability, optimal experimental data sets and computational modeling approaches should be developed as an alternative tool to yield better predictions of such rock' thermophysical properties (Ricard et al., 2011).

Computational methods based on mechanistic models are also proposed to determine indirectly thermophysical properties of rocks (Hoang, 1980; Popov et al., 2003; Khandelwal, 2011), whereas inversed methods based on Markov Chain Monte Carlo (MCMC) have been used to predict the same properties and boundary heat fluxes (e.g., Monde and Mitsutake, 2001; Fudym et al., 2008). MCMC methods use Bayesian approaches and probability density functions to describe property changes with time.

These methods use forward physical models by using differential equations subject to initial and boundary conditions. Discrepancies up to 30% still exist when the numerical predictions are compared with measurements (Cao et al., 1988; Porkhial et al., 2015; Gnanasekaran and Balaji, 2013).

Up to our knowledge, inverse methods have been rarely used for the in-situ prediction of thermal diffusivities of rocks from the transient wellbore drilling data. *1-D*, *2-D* and *3-D* simulators have been developed for other applications, such as, the SFT determination, and the prediction of temperature profiles under circulation and shut-in (e.g., Lee, 1982; Espinosa-Paredes et al., 2009; Ricard and Chanu, 2013).

The development of a new simulator for the *in-situ* prediction of the thermal diffusivity of geothermal rocks using an inversion methodology is here proposed for the first time in the literature. WELLTHER-SIM uses transient BHT_m and thermophysical properties of drilling fluids as input data. Heat conduction that occurs in the wellbore and surrounding rock-formation under fluid circulation (thermal disturbance), and shut-in conditions are modeled on a transient *3-D* formulation. The conceptual model of the simulator, the numerical algorithm and validation are outlined in this work.

2. Work methodology

2.1. Physical conceptual model

The development of WELLTHER-SIM required the analysis of heat transfer involved during the wellbore drilling. A physical model to simulate the thermal behavior of a geothermal wellbore during and after drilling was considered. The main components are depicted in Fig. 1A (which provides an axial view of the wellbore and rock-formation), whereas a radial view is shown in Fig. 1B. The physical model considers purely heat conduction at the bottom zone of the wellbore where the BHT_m's are measured. Two dynamic processes were analyzed: (i) the thermal disturbance caused by the mud circulation (Fig. 1 C), and (ii) the thermal recovery that occurs after the fluid circulation when the drilling is stopped (Fig. 1D), which is known as shut-in.

For the thermal disturbance (at the bottomhole conditions), the concept of a constant temperature anomaly to consider the cooling effect of the mud circulation to the surrounding rock was assumed, starting at the time the drill bit cuts through the depth, and ending at the time the wellbore begins the shut-in (Lachenbruch and Brewer, 1959; Jaeger, 1961). The drilling mud is considered as a well-mixed fluid, which means that it may be assumed as a perfect heat conductor. Circulation time varies from 2 to 5 h, period that enables the fluid to act as a heat sink source assuming a thermal equilibrium with the drilling bit energy, and affecting the initial temperature field of the rock-formation.

For the thermal recovery, the rock-formation acts as a heat source to the wellbore to recover the initial temperature at long shut-in times (Fig. 1D). Heat conduction is considered as the main heat transfer mechanism because the drilling mud is almost immobile at the bottomhole conditions, which allows the heat convection to be neglected (Luheshi, 1983; Shen and Beck, 1986). This process has been therefore used to predict the thermal diffusivity of the rock-formation at the bottomhole conditions.

2.1.1. Model assumptions

According to thermal disturbance and recovery, the following assumptions were considered:

1. The drilling fluid and the rock-formation are homogeneous, and isotropic but with different thermophysical properties,
2. Thermal conductivity and heat capacity of drilling fluids and rock-formation materials are constant,
3. The contact thermal resistance at the wellbore boundary is neglected,

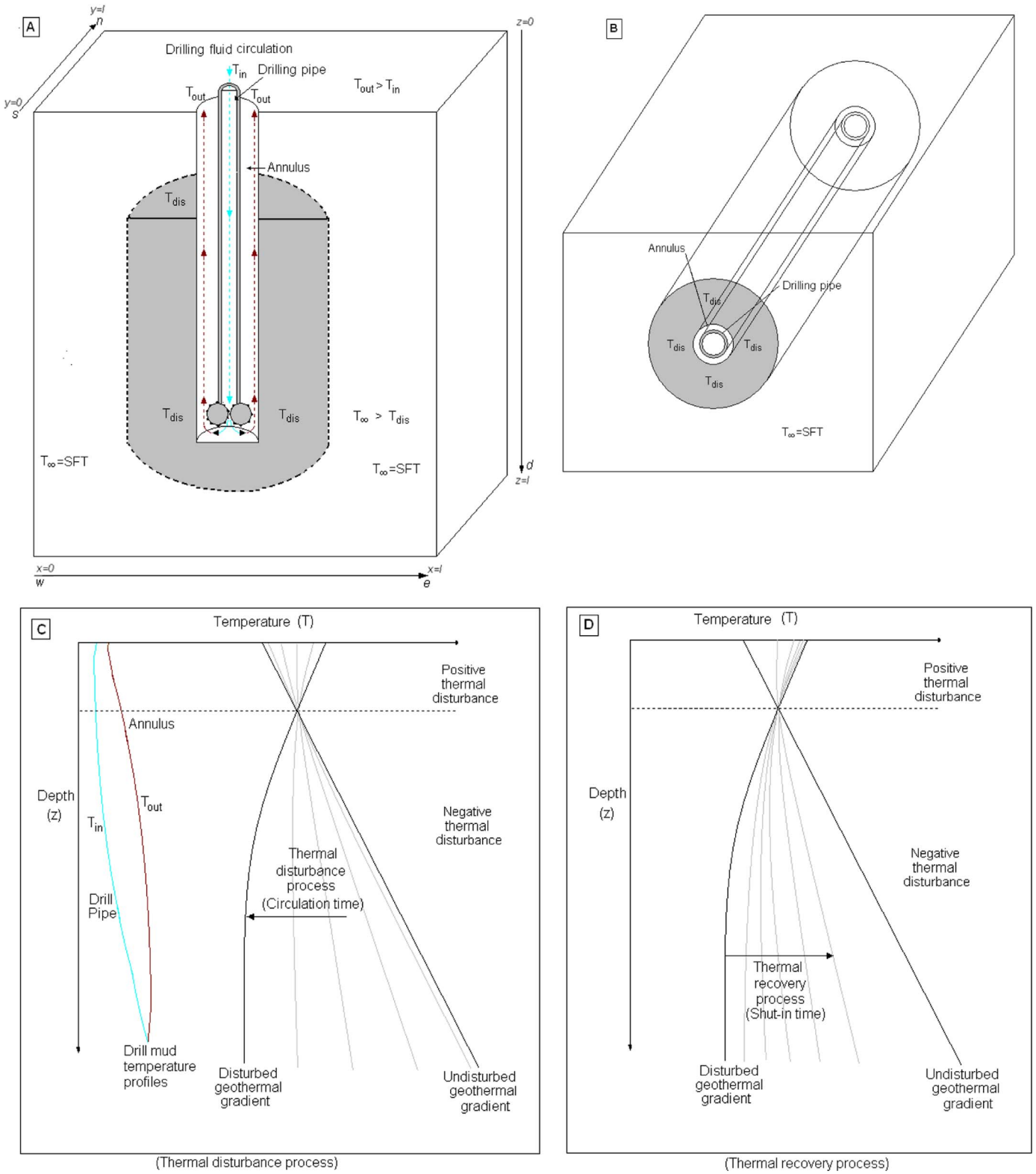

Fig. 1. Schematic representation of the *3-D* conceptual model used by WELLTHER-SIM to represent the wellbore and rock-formation system, and the heat transfer processes involved in the geothermal well drilling: (A) an axial view; (B) a radial view; (C) Thermal disturbance process; (D) Thermal recovery process. The model coordinates (*XYZ*) is also represented in the scheme (A), including their respective boundaries. T_{in}, T_{out} and T_{dis} are the inlet and outlet drilling fluid temperature, and the perturbed temperature zone, respectively.

4. The drilling fluid is considered as a heat conductor during the circulation,
5. Heat convection in the wellbore is neglected under shut-in,
6. Heat exchange between the circulating fluid and the rock-formation is treated under the condition of constant-borehole face temperature,
7. The drilling fluid is considered as an incompressible fluid,
8. No radial temperature gradient exists in the well,
9. The energy generation sources (input energy and work done by the drilling system) are neglected.

10. The initial temperature of the rock-formation is represented by the *SFT*, and
11. The temperature at the outer boundaries of the system is considered constant an equal to the *SFT*.

As a homogeneous rock-formation was assumed, the thermal diffusivities to be inferred from the simulations will correspond to average values of the geological strata where the BHT_m´*s* were measured at any wellbore depth. Regarding the assumption (9), although the input energy and work done were considered as important energy sources in a wellbore drilling system (Marshall and Bentsen, 1982), the energy generation sources were neglected and supported by the assumptions proposed by Lee (1982) and Luheshi (1983). These authors assumed that the mud circulation is used to maintain the wellbore fluid at a constant temperature, which was considered through a heat transfer to absorb most of the energy and work done by the drilling system. Because transient heat transfer was considered, the circulation time had an important effect on the mud temperature, as it absorbs most of the heat generation within the flow regions of the system due to frictional forces and the mechanical energy sources (i.e., the rotational energy due to the drill string and the drill bit). With this assumption, it considers that the RPM will reproduce the thermal recovery behavior, and hence a reliable determination of the SFT and the initial drilling mud temperature.

2.1.2. Mathematical model

A schematic diagram of the WELLTHER-SIM model used to define the orientation and the governing equations is shown in Fig. 1 A. A volumetric block of 27 m^3 (3 m x 3 m x 3 m) with a mesh-size composed by computing nodes of 3 cm x 3 cm x 3 cm was defined for the wellbore-rock system at the bottomhole conditions (Fig. 2). The simulation mesh is made by the wellbore (which is shown as the grey rectangular prism), and the following rock-formation nodes: (i) eight E nodes used for the vertices of the volumetric-block (turquoise blue), which have three major faces in contact with the boundary temperature (SFT); (ii) twelfth edge V nodes assembled at the corners (navy blue), which have two faces in contact with the boundary temperature (SFT); (iii) six C nodes represented as the main faces of the block (green), which only have a face in contact with the boundary temperature (SFT); and (iv) a variable number of inner INT nodes that will depend on the mesh-size (e.g., if the node size is 3 cm, the INT nodes will be 1×10^6), excluding the nodes that are in contact with the borehole. Additionally there are six main nodes that are in contact with the wellbore and the rock-formation, which are represented by the North, West, East, South, Upper, and Bottom faces of the rectangular prism volume of the wellbore (see the small prism at the right-bottom side of

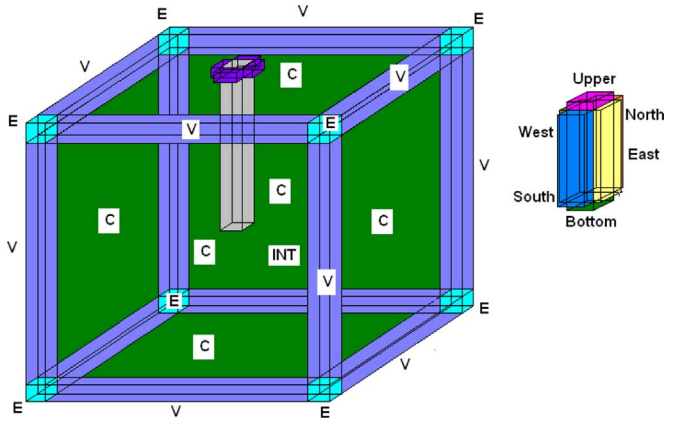

Fig. 2. Schematic diagram showing the volumetric block used by WELLTHER-SIM for representing the temperature boundaries and the computing nodes. The simulation mesh is formed by the wellbore (which is schematically represented by the grey rectangular prism volume), and the following surrounding rock-formation nodes.

Fig. 2). According to this figure, two models were used to represent the heat transfer processes: (i) the mud circulation or thermal disturbance; (ii) the thermal recovery or shut-in; which are described as follows:

(i) Thermal disturbance:

The *3-D* heat conduction equation under rectangular (*x, y, z*) coordinates and transient conditions is given as follows:

$$\frac{\partial}{\partial x}\left(k_r\frac{\partial T}{\partial x}\right)+\frac{\partial}{\partial y}\left(k_r\frac{\partial T}{\partial y}\right)+\frac{\partial}{\partial z}\left(k_r\frac{\partial T}{\partial z}\right)=\rho_r c_r\frac{\partial T}{\partial t_c} \quad (1)$$

Eq. (1) was solved by considering the mud circulation, and the wellbore as a heat sink, subject to the following conditions given by the initial temperature field of the rock-formation,

$$T(x,\ y,\ z,\ t_c{=}0) = SFT \quad (2)$$

with the following interval of rectangular coordinates:

$$0 < x{<}(c - r_w)\,and\,(c + r_w){<}x < l$$
$$0 < y{<}(c - r_w)\,and\,(c + r_w){<}y < l$$
$$c < z < l$$

and the boundary conditions given by the *SFT* (Eq. (3)); and the circulating fluid temperature (Eq. (4)):

$$T(x, y, z, t_c) = SFT \quad (3)$$

with the following interval of rectangular coordinates:

$$x = 0,\ x = l$$

$$y = 0,\ y = l$$

$$z = 0,\ z = l$$

$$\text{and,}\quad T(x, y, z, t_c) = T_{f0} \quad (4)$$

with the following interval of rectangular coordinates:

$$(c{-}r_w) < x < (c{+}r_w)$$

$$(c{-}r_w) < y < (c{+}r_w)$$

$$0 < z < c$$

where k_r, ρ_r, and c_r are the thermal conductivity, the density, and the heat capacity of the rock-formation, respectively; t_c represents the circulation time; c is the bottom hole center; r_w is the wellbore radius; and T_{f0} is the initial temperature of the circulating drilling mud.

The thermal disturbance was used as a crucial step to compute recursively the initial thermal conditions for modeling the thermal recovery process.

(ii) Thermal recovery (shut-in):

The *3-D* heat transfer equation for conduction under rectangular (*x, y, z*) coordinates and transient conditions was solved by dividing the system in two main components: (1) the rock-formation, and (2) the wellbore, according to the Eqs. (5) and (6), respectively:

$$\frac{\partial}{\partial x}\left(k_r\frac{\partial T}{\partial x}\right)+\frac{\partial}{\partial y}\left(k_r\frac{\partial T}{\partial y}\right)+\frac{\partial}{\partial z}\left(k_r\frac{\partial T}{\partial z}\right)=\rho_r c_r\frac{\partial T}{\partial t_s} \quad (5)$$

with the following interval of rectangular coordinates:

$$0 < x{<}(c - r_w)\,and\,(c + r_w){<}x < l$$
$$0 < y{<}(c - r_w)\,and\,(c + r_w){<}y < l$$
$$c < z < l$$

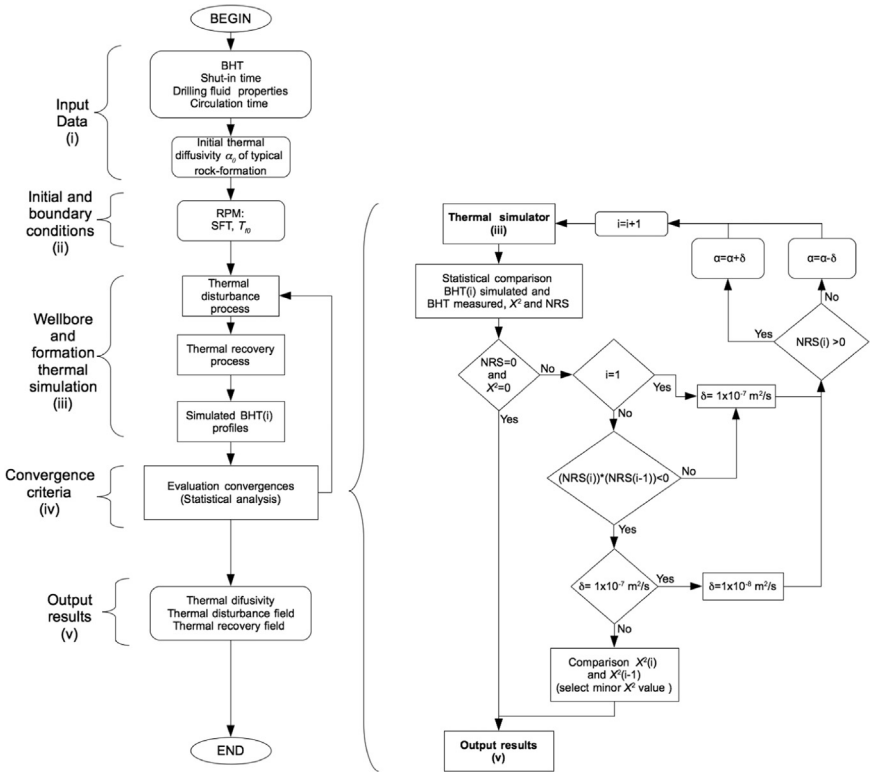

Fig. 3. Schematic flow diagram of the 3-D model showing the numerical algorithm used by WELLTHER-SIM.

and,

$$\frac{\partial}{\partial x}\left(k_f\frac{\partial T}{\partial x}\right)+\frac{\partial}{\partial y}\left(k_f\frac{\partial T}{\partial y}\right)+\frac{\partial}{\partial z}\left(k_f\frac{\partial T}{\partial z}\right)=\rho_f c_f\frac{\partial T}{\partial t_s} \tag{6}$$

with the following interval of rectangular coordinates:

$(c-r_w) < x < (c+r_w)$

$(c-r_w) < y < (c+r_w)$

$0 < z < c$

Subject to the boundary conditions given by the SFT and the shut-in time conditions for the rock-formation (Eq. (7)) and the wellbore (Eq. (8)), respectively:

$$T(x, y, z, t_s) = SFT \tag{7}$$

with the following interval of rectangular coordinates:

$x = 0,\ x = l$

$y = 0,\ y = l$

$z = 0,\ z = l$

and, $T(x, y, z, t_s{=}0) = T_{f0}$ (8)

with the following interval of rectangular coordinates:

$(c-r_w) < x < (c+r_w)$

$(c-r_w) < y < (c+r_w)$

$0 < z < c$

where k_f, ρ_f, and c_f are the thermal conductivity, the density, and the heat capacity of drilling fluid, respectively; and t_s is the shut-in time.

The initial (*SFT*) and the boundary (T_{fO}) temperature conditions were estimated by using the Rational Polynomial Method (*RPM*) proposed by Wong-Loya et al. (2015), which provided a mathematical function to describe the thermal recovery at each wellbore depth. *RPM* provides the initial drilling fluid temperature (T_{fO}) and *SFT* at zero and infinite shut-in times, respectively. This method replaces the classical Horner-plot method to infer the SFT because it systematically underestimates the *SFT* (Verma et al., 2006). RPM was applied to the BHT_m measurements under shut-in for inferring the SFT.

For solving the governing Eqs. (1, 5, and 6), the numerical technique of finite volume was used to discretize in optimized form such equations (e.g., García-Valladares, 2007). Eq. (9) shows the resulting discretized equation, which was obtained from the *3-D* model coordinates (Fig. 1 A).

$$\frac{\Delta y\Delta z}{\Delta x}(T_e-T_p)-\frac{\Delta y\Delta z}{\Delta x}(T_p-T_w)+\frac{\Delta x\Delta z}{\Delta y}(T_n-T_p)-\frac{\Delta x\Delta z}{\Delta y}(T_p-T_s)$$
$$+\frac{\Delta x\Delta y}{\Delta z}(T_b-T_p)-\frac{\Delta x\Delta y}{\Delta z}(T_p-T_u)=\frac{\rho c\Delta x\Delta y\Delta z}{k\Delta t}(T_p-T_p^0) \tag{9}$$

where T_p is the temperature of the control volume to be analyzed; T_e, T_w, T_n, T_s, T_d, and T_u are the temperature of the adjacent nodes of the mesh; T_p^0 is the temperature of the node at the preceding time step; Δx, Δy, and Δz define the mesh or node size in x, y, and z axis, respectively; Δt is the time step, ρ is the density, c is the heat capacity and k is the heat conductivity either for the drilling fluid or the rock-formation (depending on the node position).

For the calculation of the rock thermal diffusivity, Eq. (9) was simplified by substituting the thermophysical properties ρ, c, and k by α :

$$\frac{\alpha\Delta y\Delta z}{\Delta x}T_e-\frac{\alpha\Delta y\Delta z}{\Delta x}T_p-\frac{\alpha\Delta y\Delta z}{\Delta x}T_p+\frac{\alpha\Delta y\Delta z}{\Delta x}T_w+\frac{\alpha\Delta x\Delta z}{\Delta y}T_n-\frac{\alpha\Delta x\Delta z}{\Delta y}T_p$$
$$-\frac{\alpha\Delta x\Delta z}{\Delta y}T_p+\frac{\alpha\Delta x\Delta z}{\Delta y}T_s+\frac{\alpha\Delta x\Delta y}{\Delta z}T_b-\frac{\alpha\Delta x\Delta y}{\Delta z}T_p-\frac{\alpha\Delta x\Delta y}{\Delta z}T_p+\frac{\alpha\Delta x\Delta y}{\Delta z}T_u$$
$$=\frac{\Delta x\Delta y\Delta z}{\Delta t}T_p-\frac{\Delta x\Delta y\Delta z}{\Delta t}T_p^0 \tag{10}$$

The resulting set of non-linear algebraic equations was solved by an iterative numerical method based on the tridiagonal matrix algorithm (García-Valladares et al., 2004).

2.1.3. Development of the computer code

The computer code was programmed in Visual Fortran language.

Table 1
Thermal diffusivity values reported in the literature for different rock-formation types.

Rock-formation type	Thermal Diffusivity (m^2/s) x 10^{-7}	Literature source
Granodiorite	10.4	Arndt et al. (1997)
Olivine-Melilitite	8.7	Büttner et al. (1988)
Amphibolites	8.0	Seipold and Huenges (1988)
Granite	8.9	Wen et al. (2015)
Sandstone	3.7	Wen et al. (2015)
Basalt	9.4	Grirate et al. (2016)
Granite	9.3	Grirate et al. (2016)
Marble	7.5	Grirate et al. (2016)
Gabbro	11.0	Stylianou et al. (2016)
Diabase	9.0	Stylianou et al. (2016)
Andesite	4.9	Guerrero-Martinez and Verma (2013)
Dacite	9.7	Canet et al. (2015)

The numerical algorithm used is schematically shown in Fig. 3. The procedure to determine the thermal diffusivity of geothermal rocks involves five major tasks:

(i) Input data where BHT_m measurements, drilling fluid thermal properties, and drilling circulation times are entered, together with an initial approach or "guess value" for the rock-formation thermal diffusivity (α_{r1}), which is defined from the rock-formation database (Table 1).
(ii) The calculation of the initial and boundary conditions for the temperature by using the *RPM* (i.e., the *SFT* and the T_{f0}, respectively).
(iii) The numerical simulation of the thermal disturbance and the thermal recovery processes for the wellbore and the surrounding rock-formation system.
(iv) The convergence criteria where the simulated BHT_s data series are compared with those BHT_m measurements logged under shut-in: Fig. 3 (iv). At this step, the simulator iteratively decides either: (1) to correct the initial rock-formation thermal diffusivity, α_1 [by applying small decreases or increases to the approximated α_i values using the mathematical conditions imposed by the *Sum of Normalized Residuals*, *NRS*: Fig. 3 (iv)] or (2) to accept the predicted $\alpha_{r\,i+1}$ after obtaining the smallest difference among the *n*-simulated and measured *BHT* profiles of the wellbore, which is confirmed by the *NRS* and the *Chi-squared* (χ^2) statistical parameters (Eqs. (11) and (12)):

$$NRS = \sum_1^n \left(\frac{BHT_m - BHT_s}{BHT_m} \right) \tag{11}$$

$$\chi^2 = \sum_1^n \frac{(BHT_m - BHT_s)^2}{BHT_m} \tag{12}$$

As a key step of the convergence criteria (iv), the decrease or increase corrections to be applied either to the assumed initial value or the computed rock-formation thermal diffusivity will require the use of an additive correction factor (δ), which will adopt a value equal either to 1×10^{-7} or 1×10^{-8} m^2/s (when the product $NRS_{(i-1)}{}^*NRS_{(i)}$ shows a negative change) for the next iterations. This iterative procedure continues until either a new negative sign change is found or an acceptable agreement between the simulated (BHT_s) and measured (BHT_m) temperature profiles is achieved (i.e., when the statistical χ^2 and *NRS* approaches to zero, which is interpreted as the smallest difference among such temperatures).
(v) The output simulation data where the thermal diffusivity of the rock-formation is reported, including the *2-D* or *3-D* temperature fields for the thermal disturbance and recovery processes.

Table 2
Thermophysical properties of rock-formation (*r*) and drilling fluids (*f*) used by Shen and Beck (1986) to generate "experimental" (synthetic) *BHT* data series. r_w, t_c, and *SFT* are the wellbore radius, the drilling circulation time, and the static formation temperature, respectively.

Thermophysical properties	Value	Units
k_r	2.51	$\frac{W}{m\,K}$
$\rho_r c_r$	2.09	$\frac{J}{cm^3 K}$
k_f	0.61	$\frac{W}{m\,K}$
$\rho_f c_f$	4.19	$\frac{J}{cm^3 K}$
r_w	0.108	*m*
t_c	5	*h*
SFT	80	°C
T_{f0}	40	°C

2.2. Description of the validation and application cases

2.2.1. Validation case

To verify the physical model and the numerical algorithm of WELLTHER-SIM, a validation case to predict the rock-formation thermal diffusivity was formulated. An "experimental" (synthetic) BHT_m dataset proposed by Shen and Beck (1986) was used. This dataset was obtained from a numerical experiment, where the thermophysical properties of the rock-formation (*r*) and drilling fluid (*f*) were known with accuracy (Table 2). For this case, the analytical solution of the heat conduction problem given by an infinite medium bounded internally by a circular cylinder with a constant wall temperature was used (Carslaw and Jaeger, 1959).

2.2.2. Numerical application cases

Two application cases (related to medium- and high-temperature geothermal wellbores) were analyzed. For these purposes, BHT_m data sets collected from two wellbores drilled in Oguni (OGF, Japan) and Los Humeros (LHGF, Mexico) geothermal fields were used. The goal of these analyses was to predict the thermal diffusivities of the main rock-formations for the wellbores LC-1 (OGF) and LH-29 (LHGF). The location of OGF and LHGF were already cited in previous works reported in the literature (e.g., Akasaka and Nakanishi, 2000; and García-López et al., 2014; see Figs. 1 and 2, therein published, respectively).

2.2.2.1. Oguni geothermal field. The OGF is located in the central part of Kyushu Island, Southwestern Japan. Moderate deep temperatures ranging from 200 to 240 °C were measured (Abe et al., 1995). The subsurface geology of OGF consists of a thick layer of Quaternary volcanic and associated rocks, which overlie the Tertiary formations (granitic and metamorphic). Quaternary rocks mainly consist in andesitic and dacitic volcanic rocks (Yamada et al., 2000).

2.2.2.2. Los humeros geothermal field. The LHGF is situated in the Mexican Volcanic Belt within a Quaternary caldera, where the fluids are contained in andesite rocks overlying a complex basement of metamorphic, sedimentary and intrusive rocks (Luviano et al., 2015). LHGF is considered as a "super hot" geothermal system (with temperatures > 300 °C), in which around 40 deep producing wells produce high steam fractions. The wellbore LH-29 was drilled at a total depth of 2200 m, and completed in andesitic rock-formations. Deep temperatures of 300 °C (at 1300 m) and 342 °C (at 1500 m) were logged from direct measurements and fluid inclusions (as homogenization temperatures), respectively. LH-29 is currently used as a reinjection well, which is located in the central collapse area of the LHGF (Luviano et al., 2015; see Fig. 1 therein reported).

Table 3
"Experimental" (synthetic) BHT_m data series reported by Shen and Beck (1986) and simulated BHT_s data predicted from the numerical simulation carried out in this work using the WELLTHER-SIM *3-D* simulator.

Shut-in time (h)	BHT_m (°C)	BHT_s (°C)
2.5	56.6	56.6
5.0	61.3	61.7
7.5	64.3	64.8
10	66.6	67.1
15	69.6	70.1
20	71.7	71.9
30	74.1	74.2
40	75.5	75.5

3. Simulation results

3.1. Validation

As an essential test of the validation case, the thermal disturbance and recovery processes were predicted. According to the assumptions considered by Shen and Beck (1986), and to have similar conditions to be compared, the simulated BHT_s profile (predicted by WELLTHER-SIM) was computed at the wellbore wall, instead of a BHT_s profile at bottomhole conditions (which may be also computed by the simulator). Both simulated (BHT_s) and "experimental" synthetic (BHT_m) data are reported in Table 3. As can be verified, the BHT_s predicted by WELLTHER-SIM are in a good agreement with those synthetic BHT_m data reported by Shen and Beck (1986). A statistical comparison between BHT_s and BHT_m data was performed by calculating the statistical parameters (NRS=−0.033andχ^2 = 0.0145), which confirmed that the simulated BHT_s data closely matched with the reported BHT_m data using a known rock thermal diffusivity. Such a validation was also verified by means of a linear regression between BHT_s and BHT_m data (Fig. 4), which shows a very good statistical correlation given by the slope and intercept parameters, the linear correlation coefficient, and the number of regression data.

3.2. Application results - Oguni Geothermal Field (OGF)

3.2.1. Input data

Fig. 3(i). Thermal recovery data series reported for the wellbore LC-1 consists of ten measurements of *BHT* and shut-in times (Table 4), which were logged during the drilling operations (Hyodo and Takasugi, 1995). To start with the simulation, a mean value of α_f=1.46×10^{-7} m^2/s was assumed for the drilling fluid thermal diffusivity (Shen and Beck, 1986), whereas for the rock thermal diffusivity (α_r), an initial value of 6.1×10^{-7} m^2/s was assumed as the first "guess value" (α_{r1}, see Table 4). In relation to the drilling fluid circulation time (t_c), a typical value of 5 h was considered.

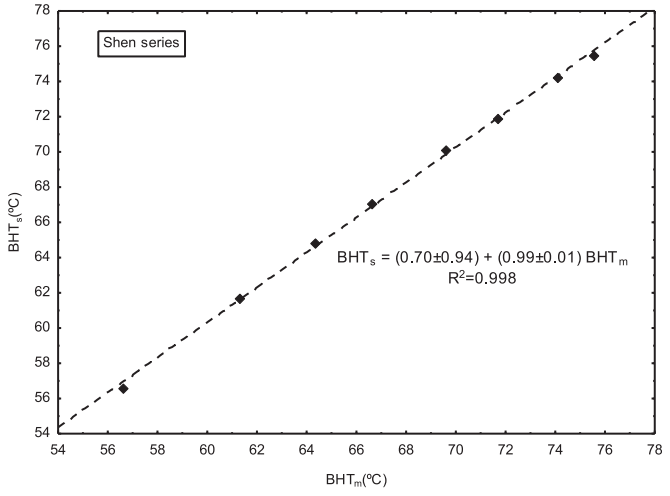

Fig. 4. Linear regression plot obtained between BHT_s (simulated in this work) and BHT_m (reported as experimental synthetic data by Shen and Beck, 1986). R^2 is a regression parameter that together with the number of data (n), expresses the statistical confidence to correlate linearly the dependent and independent variables.

3.2.2. Initial and boundary conditions

Fig. 3(ii). By applying the RPM to the LC-1 transient *BHT* data, a mathematical model was obtained (Eq. (13)) from which the initial drilling fluid temperature (T_{f0}) and the *SFT* were estimated as 55.24 ± 2.7 °C and 194.20 ± 0.06 °C, respectively. Such values represent the initial and the temperature boundary conditions for the wellbore simulation, respectively. The coefficients of Eq. (13) were used with the total number of digits indicated because of the high sensitivity of the RPM model among the possible values that may estimate for the *SFT* from a rounding-off criterion.

$$BHT\,(t) = \frac{(55.\ 237369 \pm 2.\ 6985746) + (13.\ 295306 \pm 0.\ 0002406)(t)}{1+(0.\ 0684606 \pm 9.\ 69E{-}7)(t)} \quad (13)$$

3.2.3. Thermal simulation of the wellbore and rock-formation system

Fig. 3(iii). As a result of the iterative simulation of the thermal disturbance and recovery processes, simulated temperature data (BHT_s) and thermal diffusivity of the rock-formation (α_r) were successively determined (see the iterative predictions in Table 4 and plotted in Fig. 5). The iterative simulated BHT_s data were statistically compared with those temperature measurements (BHT_m) logged for the wellbore LC-1 by using the convergence algorithm shown in Fig. 3(iv).

As an illustrative example, for the initial-iterative simulation (i=1), χ^2 and NRS parameters were calculated as χ_1^2=3. 210 and NRS_1=0.515, respectively (see column 3 of the Table 4). The analysis of this χ_1^2value indicates a poor agreement between the simulated $BHT_{s\text{-}1}$ and measured BHT_m data (see the dashed-red curved line represented for the initial iteration α_{r1}: Fig. 5), whereas the positive value obtained for the NRS_1 shows an underestimated prediction of the actual BHT_m data. The interpretation of these statistical parameters shows that the initial guess value for the rock-formation thermal diffusivity did not satisfy the ideal convergence criteria (i.e., $\chi^2 \rightarrow 0$ and $NRS \rightarrow 0$). Therefore, a new iterative value for the rock-formation thermal diffusivity (i.e., α_{ri+1}) requires to be assumed for continuing with the simulation until to achieve the convergence [see Fig. 3(iv)]. The thermal diffusivity values of the rock-formation assumed in each iterative simulation are reported in Table 4. As a result of these sequential approaches, and the corresponding modeling of thermal processes in the wellbore and rock-formation system, simulated BHT_s values were iteratively determined (from 1 to n-iterations), and newly evaluated by using the $\chi_i^2$and NRS_i parameters until the best values of convergence were achieved (i.e., $\chi^{2,*} \rightarrow 0$ and $NRS^* \rightarrow 0$).

For the particular case of the LC-1, five numerical iterations were required to achieve the best estimation of the simulated BHT_s data set (using ~5.5 h of CPU time with a personal computer, 2.9 GHz Intel core i7, 8 GB RAM memory), which was successfully obtained in the iteration i=4 (χ_4^2=0. 058 and NRS_4=−0.002). From this simulated data set ($BHT_{s\text{-}4}$), the convergence value for the rock-formation thermal diffusivity was finally achieved (referred as the $\alpha_{r\text{-}4}$ and reported in the column 6 of the Table 4). A summary of the complete iteration process obtained for the statistical comparison between BHT_s and BHT_m is graphically represented in Fig. 6, whereas the results for the statistical parameters χ_i^2 and NRS_i are respectively plotted in Figs. 6 A and B.

Table 4
BHT_m logged data series and simulated BHT_s data series (obtained from WELLTHER-SIM) for the wellbore LC-1 drilled in the OGF.

Shut-in time (h)	BHT_m (°C)	BHT_s (°C) i=1 α_1=6.1	BHT_s (°C) i=2 α_2=7.1	BHT_s (°C) i=3 α_3=8.1	**BHT_s (°C) i=4 α_4=8**	BHT_s (°C) i=5 α_5=7.9
5.5	92.0	88.41	91.48	94.32	**94.05**	93.77
6.5	98.5	92.64	95.92	98.92	**98.63**	98.34
7.5	103.0	96.54	99.98	103.08	**102.79**	102.49
8.5	107.0	100.16	103.70	106.88	**106.58**	106.27
9.5	110.0	103.53	107.15	110.36	**110.06**	109.75
12.5	119.0	112.37	116.08	119.31	**119.01**	118.70
15.5	126.6	119.70	123.38	126.54	**126.24**	125.94
18.5	132.8	125.88	129.46	132.51	**132.23**	131.94
24.5	142.4	135.69	139.02	141.80	**141.54**	141.28
72.5	170.9	167.29	169.06	170.47	**170.35**	170.22
χ^2		3.210	0.672	0.067	**0.058**	0.064
NRS		0.515	0.227	−0.026	**−0.002**	0.022

All the thermal diffusivities (α_r) must be multiplied by the factor 10^{-7} m^2/s, and later used as approach in each computing iteration (i).

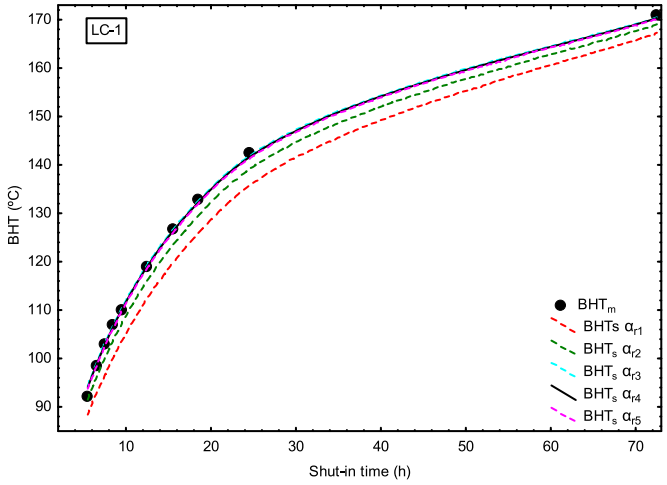

Fig. 5. Simulated transient temperature (BHT_s) profiles obtained from WELLTHER-SIM at different rock-formation thermal diffusivities by using the logged thermal recovery history (BHT_m) of the wellbore LC-1.

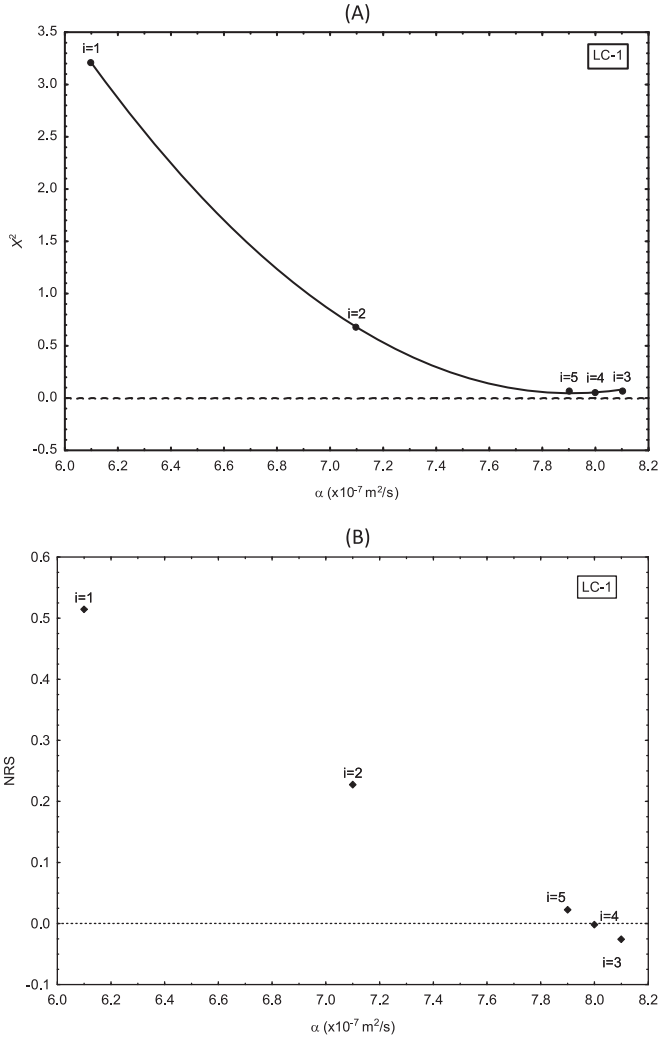

Fig. 6. Numerical evolution of the statistical parameters χ^2 (*A*)and *NRS* (*B*) computed for demonstrating the convergence of the method developed using the simulation results of the heat transfer processes (thermal disturbance and recovery) involved during the drilling operations of the wellbore LC-1.

3.3. Application results - Los Humeros Geothermal Field (LHGF)

3.3.1. Input data

The transient thermal recovery data sets reported for the LH-29 are represented by six measurements of BHT_m and shut-in times, which were logged under shut-in (Verma et al., 2006). For the analysis of the LH-29, a mean value of α_f =1.46×10^{-7} m^2/s was used for the fluid thermal diffusivity (Shen and Beck, 1986), whereas for the rock-formation (α_r), an initial value ($\alpha_{r\text{-}I}$) of 5.0×10^{-7} m^2/s was also assumed (Table 5). For the circulation time of drilling mud (t_c), the same value of 5 h was used.

3.3.2. Initial and boundary conditions

Fig. 3(ii). By a systematic application of the RPM to LH-29 transient BHT_m data, the mathematical model given by the Eq. (14) was derived for estimating the initial temperature of the drilling mud (T_{f0}) and the *SFT*, which adopted the values of 126.91 ± 8.74 °C and 296.70 ± 0.0024 °C, respectively. Such estimates acted as the initial and the boundary conditions of temperature for the simulation of the LH-29, respectively.

$$BHT(t) = \frac{(126.91 \pm 8.74) + (15.9659 \pm 1.04E{-}04)(t)}{1{+}(5.38141E{-}7)(t)} \quad (14)$$

3.3.3. Thermal simulation of the wellbore and rock-formation

Fig. 3(iii). For the thermal modeling of disturbance and recovery processes in the LH-29 and the surrounding rock-formation, simulated temperature data (BHT_s) and the thermal diffusivity of the rock-formation (α_r) were determined. These calculations are reported in Table 5 and plotted in Fig. 7. By applying the same methodology described in Fig. 3, simulated BHT_s (obtained from iterative simulations) were statistically compared with LH-29 measured data (BHT_m) using the same convergence algorithm [Fig. 3(iv)].

Table 5
BHT_m logged data series and simulated BHT_s data series (obtained from WELLTHER-SIM) for the wellbore LH-29 drilled in the LHGF.

Shut-in time (h)	BHT_m (°C)	BHT_s (°C) *i=1* α_1=5	BHT_s (°C) *i=2* α_2=6	BHT_s (°C) *i=3* α_3=5.9	BHT_s (°C) *i=4* α_4=5.8	**BHT_s (°C) *i=5* α_5=5.**	BHT_s (°C) *i=6* α_5=5.6
6	167.01	165.60	169.88	169.46	169.05	**168.63**	168.21
12	195.78	189.45	194.72	194.23	193.73	**193.22**	192.70
18	210.06	206.37	211.69	211.20	210.70	**210.20**	209.68
24	221.73	218.92	223.99	223.53	223.06	**222.58**	222.09
30	231.87	228.54	233.28	232.85	232.41	**231.96**	231.51
36	239.06	236.11	240.51	240.11	239.71	**239.29**	238.87
χ^2		0.401	0.108	0.078	0.059	**0.053**	0.059
NRS		0.098	−0.042	−0.029	−0.016	**−0.003**	0.011

Thermal diffusivities (E^{-7} m^2/s) used as approach value for each iteration (*i*).

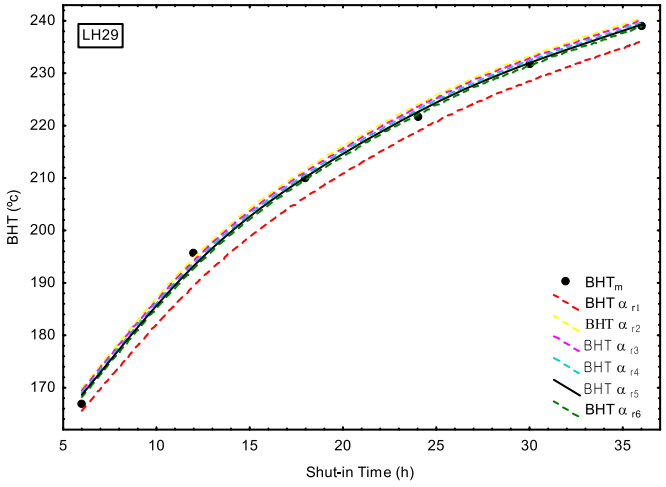

Fig. 7. Simulated transient temperature (BHT_s) profiles obtained from WELLTHER-SIM at different rock-formation thermal diffusivities by using the logged thermal recovery history (BHT_m) of the wellbore LH-29.

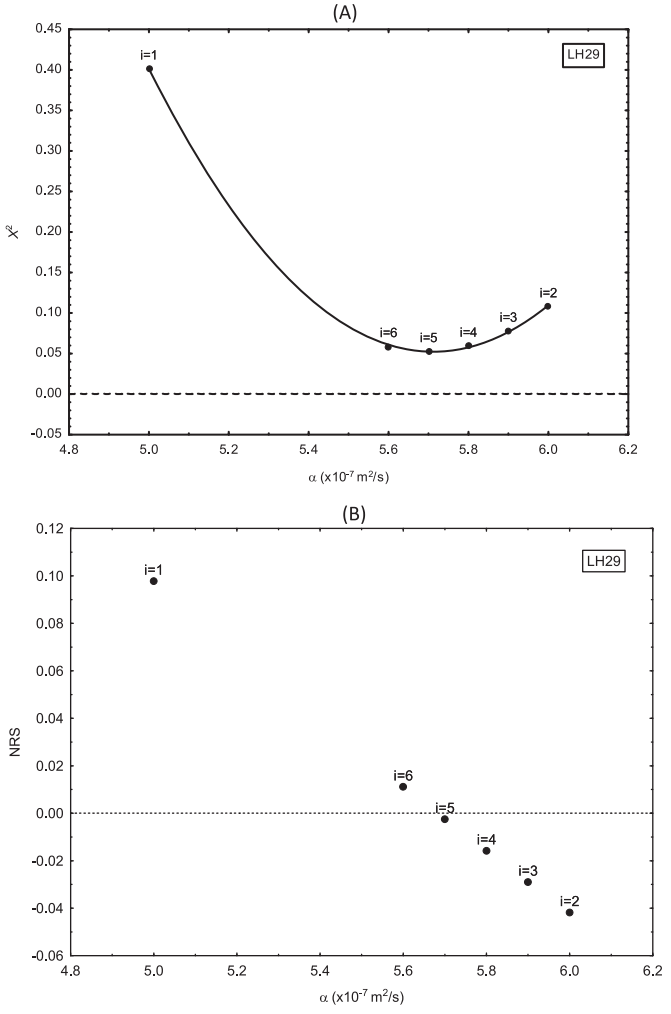

Fig. 8. Numerical evolution of the statistical parameters χ^2 (*A*)and *NRS* (*B*) computed for demonstrating the convergence of the method developed using the simulation results of the heat transfer processes (thermal disturbance and recovery) involved during the drilling operations of the wellbore LH-29.

From the initial iteration (*i*=1), χ_1^2 and NRS_1 parameters were estimated as 0.401 and 0.098, respectively (see column 3 of the Table 5). The analysis of $\chi_1^2$and NRS_1 for the LH-29 (using the first "guess value" α_{r1}=5.0×10^{-7} m^2/s) shows the same behavior obtained for the first iterative simulation of the LC-1 (OGF) case (i.e., a partial agreement between simulated and measured *BHT* data, in common with an underestimation of the BHT_m data, respectively). By following the convergence algorithm, the initial value of the rock formation diffusivity was iteratively changed by using six possible values, which are compiled in Table 5. After the sequential approaches and their thermal modeling of the same disturbance and recovery processes, simulated BHT_s values were estimated together with their respective χ_1^2 and NRS_1 parameters until the best approaches were reached (i.e., $\chi^{2,*}\rightarrow 0$ and NRS* → 0).

For the LH-29 case, six numerical iterations were required to achieve the best estimation of the simulated BHT_s data set (using ~6 h of CPU time with the same personal computer configuration), which was successfully reached in the iteration *i*=5 (χ_5^2=0. 053 and NRS_5=−0.003). From these simulated data ($BHT_{s\text{-}5}$), the convergence value for the rock-formation thermal diffusivity was achieved (referred as the α_{r5} and reported in the column 7 of the Table 5). A summary of the full iterative process obtained for the statistical comparison between BHT_s and BHT_m is shown in Fig. 7, whereas the results for the statistical parameters $\chi_i^2$and NRS_i are respectively plotted in Fig. 8 A and B.

4. Discussion of results

After revising the approaches predicted for the thermal diffusivities of the rock-formations of the LC-1 ($\alpha_{LC\text{-}1}$ =8×10^{-7} m^2/s), and LH-29 ($\alpha_{LH\text{-}29}$ =5.7×10^{-7} m^2/s), it was observed that these thermal diffusivities are in good agreement with those experimental data reported by Wen et al. (2015) and Guerrero-Martínez and Verma (2013) for granite (α_g =8.9×10^{-7} m^2/s) and andesite (α_a =4.9×10^{-7} m^2/s) rocks, respectively.

These rock-formations are referred because they are found in the geological strata of the two geothermal wellbores analyzed (LC-1 and LH-29), as can be observed in the lithostratigraphic units reported by Yamada et al. (2000) and Martínez-Serrano and Alibert (1994), respectively. In relation to the predicted values of the thermal

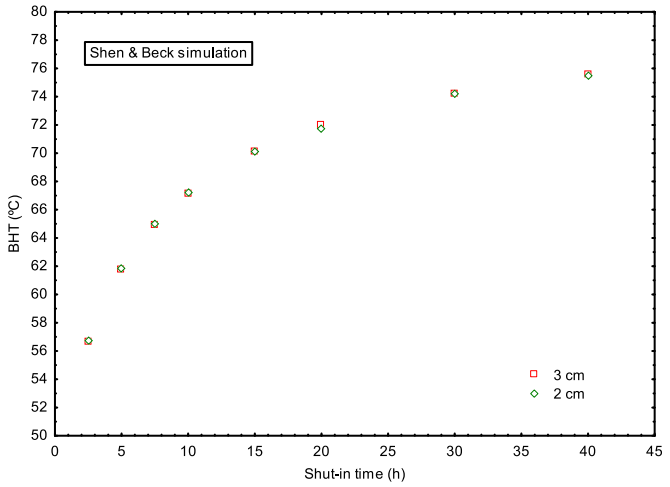

Fig. 9. Results of the mesh independence analysis obtained for the Shen and Beck validation case using 2 cm and 3 cm of mesh-size.

diffusivity for the rocks found in these geothermal sites, typical values reported in the literature were used to compare against these estimates.

Pritchett and Garg (1995) indirectly reported experimental values for thermal diffusivity of some drill cores collected in a wide range of rock-formations of the OGF, which ranged from 8.1×10^{-7} to 14.1×10^{-7} m^2/s. These values are in agreement with the WELLTHER-SIM predicted estimates of the thermal diffusivity of rocks for this geothermal site. Additionally, García et al. (1991) measured, for the first time, the thermal diffusivity of some drill cores collected from drilled wells of LHGF. By analyzing experimental transient temperature rises, caused by a line source of heat of constant strength placed along the axis of core samples, these authors reported values of thermal diffusivity of 5.4×10^{-7} m^2/s, which are in good agreement with those values inferred from the inverse method here proposed.

An additional remark of these numerical simulations is the *SFT* values obtained from this simulation study, which were successfully predicted by using the RPM. Such *SFT´s* (i.e., $SFT_{LC\text{-}1}$ =194.2 °C; $SFT_{LH\text{-}29}$ =296.7 °C) are also in agreement with some previous values reported in the literature by using alternative methods (e.g., $SFT_{LC\text{-}1}$ =200 °C reported by Abe et al., 1995; and $SFT_{LH\text{-}29}$ =300 °C reported in direct measurements by Luviano et al., 2015).

The thermal disturbance and recovery processes of these two geothermal wellbores (LC-1 and LH-29) were successfully estimated by using the WELLTHER-SIM capability and the convergence values of the rock-formation thermal diffusivities. This was consistently verified through the statistical parameters of $\chi^2$and *NRS* (LC-1: χ^2_4=0. 058 and NRS_4=−0.002; and LH-29: χ^2_5=0. 053 and NRS_5=−0.003). These results were obtained in CPU times that range from 4 h for a mesh-size of 3 cm with 1×10^6 computing nodes to 24 h for a smaller mesh-size of 2 cm with 3.3×10^6 nodes (Fig. 9), which demonstrated the stability and efficiency of the WELLTHER-SIM. As a mesh independence analysis, the numerical stability of the simulation runs was evaluated by using two different mesh-sizes (2 cm and 3 cm), which provided differences less than 0.5% in the predicted results (Fig. 9). This feature constitutes an attractive advantage of this method over complex experimental analyses to determine an *in-situ* reliable prediction of the thermal diffusivity of rocks.

The computer code of the simulator, a sample data file, and a quick user´s manual are available for downloading from the following computing repository: http://geosw.ier.unam.mx/Welltherm-sim/, which may be accessed after requesting to the authors the username and password information.

5. Conclusions

A *3-D* wellbore thermal simulator WELLTHER-SIM was developed for the *in-situ* and reliable determination of thermal diffusivities of geothermal rock-formations. The heat conduction model used enabled the drilling fluid circulation and shut-in processes to be accurately described in the wellbore and the surrounding rock-formation.

The new inverse method was validated, and applied to the analysis of two drilled wellbores of the OGF (LC-1) and LHGF (LH-29). After a small number of iterations, the simulated BHT_s data predicted by WELLTHER-SIM were in agreement with those temperature measurements (BHT_m). The rock-formation thermal diffusivities predicted for the LC-1 and LH-29 wellbores were fairly consistent with those experimental data reported for similar rock-types found in the lithological strata of each wellbore.

A good numerical stability of the simulator to predict the rock-thermal diffusivity using either close or very far initial guess values was found. This result constitutes an important convergence feature of the simulator computing processing together with the efficiency and accuracy. The numerical stability was efficiently found at different grid sizes of the *wellbore-rock system*. Finally, the successful prediction of the rock thermal diffusivities makes a practical and original scientific contribution for the geothermal industry.

Acknowledgments

The authors want to thank to DGAPA-PAPIIT (UNAM) Project IT101014 for the partial financial support, and to A. Quiroz for helping with the creation of the computer repository. The first author wants to thank the Escuela Nacional Colegio de Ciencias y Humanidades for the partial financial support. The second author also acknowledges the CONACyT (Mexico) and the CIICAp-UAEM for their financial and infrastructure support in a sabbatical leave program carried out from February 2016 to January 2017.

Appendix A. Supporting information

Supplementary data associated with this article can be found in the online version at doi:10.1016/j.cageo.2017.03.016.

References

Abe, M., Yamada, M., Kawano, Y., Todaka, N., Tezuka, S., 1995. Development of the Oguni geothermal field, Japan. In: Proceedings World Geothermal Congress 1995, Florence, Italy, pp. 1319–1322.

Akasaka, C., Nakanishi, S., 2000. Evaluation of microgravity background at the undisturbed Oguni geothermal field, Japan. In: , Proceedings of the Twenty-Fifth Workshop on Geothermal Reservoir Engineering Stanford University, Stanford, California, January 24-26, 2000 SGP-TR-165.

Arias-Penas, D., Castro-García, M.P., Rey-Ronco, M.A., Alonso-Sánchez, T., 2015. Determining the thermal diffusivity of the ground based on subsoil temperatures. Preliminary results of an experimental geothermal borehole study Q-THERMIE-UNIOVI. Geothermics 54, 35–42.

Arndt, J., Bartel, T., Scheuber, E., Schilling, F., 1997. Thermal and rheological properties of granodioritic rocks from the Central Andes, North Chile. Tectonophysics 271, 75–88.

Beck, A.E., 1988. Thermal properties. In: Haenel, R., Rybach, L., Stegena, L. (Eds.), Handbook of Terrestrial Heat- Flow Density Determination. Springer, 87–165.

Bording, T.S., Nielsen, S.B., Balling, N., 2016. The transient divided bar method for laboratory measurements of thermal properties. Geophys. J. Int. 207 (3), 1446–1455.

Büttner, R., Zimanowski, B., Blumm, J., Hagemann, L., 1988. Therm. Conduct. a Volcan. Rock. Mater. (olivine-melilitite) Temp. range 288 1470 K. J. Volcanol. Geother. Res. 80, 293–302.

Canet, C., Trillaud, F., Prol-Ledesma, R.M., González-Hernández, G., Peláez, B., Hernández-Cruz, B., Sánchez-Córdova, M.M., 2015. Thermal history of the Acoculco geothermal system, eastern Mexico: insights from numerical modeling and radiocarbon dating. J. Volcanol. Geother. Res. 305, 56–62.

Cao, S., Hermanrud, C., Lerche, I., 1988. Estimation of formation temperature from bottom-hole temperature measurements: Cost ♯1 well, Norton Sound, Alaska. Geophysics 53 (12), 1619.

Carslaw, H.S., Jaeger, J.C., 1959. Conduction of Heat in Solids. Oxford University Press.
Cloetingh, S.A.P.L., Van Wees, J.D., Ziegler, P.A., Lenkey, L., Beekman, F., Tesauro, M., Bonté, D., 2010. Lithosphere tectonics and thermo-mechanical properties: an integrated modelling approach for Enhanced Geothermal Systems exploration in Europe. Earth-Sci. Rev. 102 (3), 159–206.
Espinosa-Paredes, G., Garcia, A., Santoyo, E., Hernandez, I., 2001. TEMLOPI/V. 2: a computer program for estimation of fully transient temperatures in geothermal wells during circulation and shut-in. Comput. Geosci. 27, 327–344.
Espinosa-Paredes, G., Morales-Díaz, A., Olea-González, U., Ambriz-Garcia, J.J., 2009. Application of a proportional-integral control for the estimation of static formation temperatures in oil wells. Mar. Pet. Geol. 26 (2), 259–268.
Fuchs, S., Balling, N., Förster, A., 2015. Calculation of thermal conductivity, thermal diffusivity and specific heat capacity of sedimentary rocks using petrophysical well logs. Geophys. J. Int. 203 (3), 1977–2000.
Fudym, O., Orlande, H.R.B., Bamford, M., Batsale, J.C., 2008. Bayesian approach for thermal diffusivity mapping from infrared images with spatially random heat pulse heating. J. Phys. Conf. Series 135, 12042.
García, A., Contreras, E., Domínguez, B., 1991. Developments in geothermal energy in Mexico—part thirty-three. Simultaneous determination of the thermal properties of geothermal drill cores. Heat. Rec. Sys. CHP 11 (2–3), 131–139.
García, A., Santoyo, E., Espinosa, G., 1998. Estimation of temperatures in geothermal wells during circulation and shut-in in the presence of lost circulation. Transp. Porous Media 33, 103–127.
García-López, C.G., Pandarinath, K., Santoyo, E., 2014. Solute and gas geothermometry of geothermal wells: a geochemometrics study for evaluating the effectiveness of geothermometers to predict deep reservoir temperatures. Int. Geol. Rev. 56 (16), 2015–2049.
García-Valladares, O., 2007. Numerical simulation of non-adiabatic capillary tubes considering metastable region. Part I: Mathematical formulation and numerical model. Int. J. Refrig. 30, 642–653.
García-Valladares, O., Pérez-Segarra, C.D., Rigola, J., 2004. Numerical simulation of double-pipe condensers and evaporators. Int. J. Refrig. 27, 656–670.
Gibert, B., 2003. Thermal diffusivity of upper mantle rocks: influence of temperature, pressure, and the deformation fabric. J. Geophys. Res. 108 (B8), 1–15.
Gnanasekaran, N., Balaji, C., 2013. Markov Chain Monte Carlo (MCMC) approach for the determination of thermal diffusivity using transient fin heat transfer experiments. Int. J. Therm. Sci. 63, 46–54.
Grirate, H., Agalit, H., Zari, N., Elmchaouri, A., Molina, S., Couturier, R., 2016. Experimental and numerical investigation of potential filler materials for thermal oil thermocline storage. Sol. Energy 131, 260–274.
Guerrero-Martínez, F.J., Verma, S.P., 2013. Three dimensional temperature simulation from cooling of two magma chambers in the Las Tres Vírgenes geothermal field, Baja California Sur, Mexico. Energy 52, 110–118.
Hoang, V.T., 1980. Estimation of In-situ Thermal Conductivities from Temperature Gradient Measurements (PhD Thesis). Lawrence BerkeleyLaboratory, University of California, USA.
Hyodo, M., Takasugi, S., 1995. Evaluation of the curve-fitting method and the Horner-plot method for estimation of the true formation temperature using temperature recovery logging data. In: Proceedings of the 20th Workshop on Geothermal Reservoir Engineering Stanford University, Stanford, USA, pp. 94–100.
Jaeger, J.C., 1961. The effect of the drilling fluid on temperatures measured in bore holes. J. Geophys. Res. 66, 563–569.
Khandelwal, M., 2011. Prediction of thermal conductivity of rocks by soft computing. Int. J. Earth Sci. 100, 1383–1389.
Kiyohashi, H. Matsuki, A., Takasugi S., 1996. Measurement of thermal conductivity of bentonite mud at high temperatures and pressures. In: Proceedings 8th International Symp. Observation of the Continental Crust through Drilling, Tsukuba, Japan, 337–342.
Krishnaiah, S., Singh, D., Jadhav, G., 2004. A methodology for determining thermal properties of rocks. Int. J. Rock. Mech. Min. Sci. 41, 877–882.
Lachenbruch, A.H., Brewer, M.C., 1959. Dissipation of the temperature effect of drilling a well in arctic Alaska. Bulletin of the USGS1083-C. Government Printing Office, 73–109.
Lee, T.C., 1982. Estimation of formation temperature and thermal property from dissipation of heat generated by drilling. Geophysics 47, 1577–1584.
Li, M., Liu, G., Li, J., Zhang, T., He, M., 2015. Thermal performance analysis of drilling horizontal wells in high temperature formations. Appl. Therm. Eng. 78, 217–227.
Liu, C., Chen, Y., Li, K., 2016. Static formation temperature prediction based on bottom hole temperatures. In: Proceedings of the 41st Workshop on Geothermal Reservoir Engineering, Stanford University, Stanford, USA, 13 p.
Luheshi, M.N., 1983. Estimation of formation temperature from borehole measurements. Geophys. J. Int. 74, 747–776.
Luviano, M.S., Armenta, M.F., Montes, M.R., 2015. Thermal Stimulation to Improve the Permeability of Geothermal Wells in Los Humeros Geothermal Field, Mexico. In: Proceedings World Geothermal Congress Melbourne, Australia, 19-25 April 201, 10 p.
Marshall, D.W., Bentsen, R.G., 1982. Computer model to determine the temperature distributions in a wellbore. J. Can. Petrol. Tech. 21 (1), 63–75.
Martínez-Serrano, R., Alibert, C., 1994. Características geoquímicas delas rocas volcánicas del sistema geotérmico Los Humeros. Puebla Y. su relación con la Mineral. De. Alter. Geofís. Int. 4, 585–605.
Monde, M., Mitsutake, Y., 2001. A new estimation method of thermal diffusivity using analytical inverse solution for one-dimensional heat conduction. Int. J. Heat. Mass Trans. 44 (16), 3169–3177.
Popov, Y., Tertychnyi, V., Romushkevich, R., Korobkov, D., Pohl, J., 2003. Interrelations between thermal conductivity and other physical properties of rocks: experimental dataThermo-Hydro-Mechanical Coupling in Fractured Rock, Birkhäuser Basel, 1137–1161.
Porkhial, S., Salehpourb, M., Ashrafc, H., Jamalic, A., 2015. Modeling and prediction of geothermal reservoir temperature behavior using evolutionary design of neural networks. Geothermics 53, 320–327.
Pritchett, J.W., Garg, S.K., 1995. A modeling study of the Oguni geothermal field, Kyushu, Japan. In: Proceedings World Geothermal Congress '95, Florence pp. 18–31.
Ricard, L.P., Chanu, J.B., 2013. GeoTemp™ 1.0: a MATLAB-based program for the processing, interpretation and modelling of geological formation temperature measurements. Comput. Geosci. 57, 197–207.
Ricard, L.P. Esteban, L., Pimienta, L., Delle Piane, C., Evans, C., Chanu, J.-.B., Sarout, J., 2011. Temperature estimates for geothermal application: Cockburn 1, Perth Basin, Australia. In Australian Geothermal Energy Conference 2011, pp. 1–6.
Santoyo, E., García, A., Morales, J.M., Contreras, E., Espinosa-Paredes, G., 2001. Effective thermal conductivity of Mexican geothermal cementing systems in the temperature range from 28°C to 200°C. Appl. Therm. Eng. 21, 1799–1812.
Santoyo, E., García, A., Espinosa, G., Santoyo-Gutiérrez, S., González-Partida, E., 2003. Convective heat-transfer coefficients of non-Newtonian geothermal drilling fluids. J. Geochem. Expl. 78, 249–255.
Sass, J.H., Stone, C., Munroe, R.J., 1984. Thermal conductivity determinations on solid rock—a comparison between a steady-state divided-bar apparatus and a commercial transient line-source device. J. Volcanol. Geother. Res. 20, 145–153.
Seipold, U., Huenges, E., 1988. Thermal properties of gneisses and amphibolites high pressure and high temperature investigations of KTB-rock samples. Tectonophysics 291, 173–178.
Shen, P.Y., Beck, A.E., 1986. Stabilization of bottom hole temperature with finite circulation time and fluid flow. Geophys. J. Int. 86, 63–90.
Stylianou, I., Tassou, S., Christodoulides, P., Panayides, I., Florides, G., 2016. Measurement and analysis of thermal properties of rocks for the compilation of geothermal maps of Cyprus. Renew. Energy 88, 418–429.
Sundberg, J., Back, P.E., Ericsson, L.O., Wrafter, J., 2009. Estimation of thermal conductivity and its spatial variability in igneous rocks from in situ density logging. Int. J. Rock. Mech. Min. Sci. 46 (6), 1023–1028.
Tommasi, A., Gibert, B., Seipold, U., Mainprice, D., 2001. Anisotropy of thermal diffusivity in the upper mantle. Nature 411, 783–786.
Verma, S.P., Andaverde, J., Santoyo, E., 2006. Statistical evaluation of methods for the calculation of static formation temperatures in geothermal and oil wells using an extension of the error propagation theory. J. Geochem. Explor. 89, 398–404.
Vosteen, H.D., Schellschmidt, R., 2003. Influence of temperature on thermal conductivity, thermal capacity and thermal diffusivity for different types of rock. Phys. and Chem. Earth, Parts A/B/C. 28 (9), 499–509.
Weirich, J.B., Bland, R.G., Smith Jr, W.W., Krueger, V., Harrell, J.W., Nasr, H.N., Papanyan, V., 2001. U.S. Patent No. 6,176,323. Washington, DC: U.S. Patent and Trademark Office.
Wen, H., Lua, j., Xiao, Y., Denga, J., 2015. Temperature dependence of thermal conductivity, diffusion and specific heat capacity for coal and rocks from coal field. Thermochim. Acta 619, 41–47.
Whittington, A.G., Hofmeister, A.M., Nabelek, P.I., 2009. Temperature-dependent thermal diffusivity of the Earth's crust and implications for magmatism. Nature 458 (7236), 319–321.
Wohletz, K., Civetta, L., Orsi, G., 1999. Thermal evolution of the Phlegraean magmatic system. J. Volcanol. Geother. Res. 91 (2), 381–414.
Wong-Loya, J.A., Santoyo, E., Andaverde, J.A., Quiroz-Ruiz, A., 2015. RPM-WEBBSYS: a web-based computer system to apply the rational polynomial method for estimating static formation temperatures of petroleum and geothermal wells. Comput. Geosci. 85, 45–59.
Wu, B., Zhang, X., Jeffrey, R.G., 2014. A model for downhole fluid and rock temperature prediction during circulation. Geothermics 50, 202–212.
Yamada, M., Iguchi, K., Nakanishi, S., Todaka, N., 2000. Reservoir characteristics and development plan of the Oguni geothermal field, Kyushu, Japan. Geothermics. http://dx.doi.org/10.1016/S0375-6505(99)00058-9.
Yang, M., Meng, Y., Li, G., Li, Y., Chen, Y., Zhao, X., Li, H., 2013. Estimation of wellbore and formation temperatures during the drilling process under lost circulation conditions. Mathe. Probl. Eng., 1–12, (Article No. 579091).
Zhou, F., Xiong, Y., Tian, M., 2015. Predicting initial formation temperature for deep well engineering with a new method. J. Earth Sci. 26, 108–115.